Low and high Reynolds number flows inside Taylor cones

A. Barrero, A. M. Gañán-Calvo, J. Dávila, A. Palacio, and E. Gómez-González
Escuela Superior de Ingenieros, Universidad de Sevilla, Camino de los Descubrimientos s/n, 41012 Sevilla, Spain
(Received 15 June 1998)

Liquid motions inside Taylor cones exhibit interesting features which are not well understood yet. In addition to the flow rate injected through the electrified needle to which the conical meniscus is anchored, the action of the tangential electrical stress on the cone surface induces a recirculating meridional motion, towards the apex along the generatrix and away from it along the axis. Sometimes, a vigorous swirl is observed. The characteristic value of the liquid velocity is found to be highly dependent on both the electrical conductivity and the viscosity of the liquid, so that the Reynolds number of the liquid flow varies from very small values (creeping flow) for the case of highly conducting and viscous liquids to relatively large values for liquids with sufficiently low values of the liquid conductivity and viscosity. Theoretical conical flows for low and high values of the Reynolds number show qualitatively good agreement with photographs of real flows inside Taylor cones. In particular, the existence of a vigorous swirl which is observed in the electrospraying of paraffins and other poorly conducting and low viscosity liquids can be explained as bifurcation of a primarily nonswirling meridional flow when the Reynolds number reaches a critical value. [S1063-651X(98)01512-8]

PACS number(s): 47.15.Gf, 47.20.Ky, 47.65.+a, 47.32.Cc

I. INTRODUCTION

Electrostatic atomization (electrospray) when operating in the so-called cone-jet mode [1] is a very useful technique to generate monodispersed aerosols with droplet diameters in the range of tens of nanometers to hundreds of microns. In spite of the existence of other competing mechanical techniques to generate monodispersed aerosols in the micrometric range [2,3], electrosprays are still attractive in that range since they exhibit some other interesting properties such as a high surface charge of the generated droplets or the fact that the droplet diameter can be easily controlled by varying either the electrosprayed flow rate or the electrical conductivity of the liquid sample. Because of their properties, electrosprays have applications to processes such as production of ceramic powders, production of aerosol standards, mass spectrometry [4–7], etc.

Usually, the electroatomization technique consists in the injection of a liquid through a capillary, electrified needle. For a certain range of values of both the applied voltage and the injected flow rate, the electrified meniscus adopts an almost conical shape. Charge and mass are emitted from the cone vertex in the form of an extremely thin, capillary, charged jet that eventually breaks up into a fine spray with the above-mentioned distinctive characteristics.

From the pioneering experimental work by Zeleny [8,9] much is known about electrospray physics. In a famous paper [10], Taylor gave an explanation of the conical shape of electrified menisci for perfectly conducting liquids. Much more recently, several theoretical and experimental studies have contributed to increasing the knowledge of the electrospray phenomenon [11–19]. In particular, the dependence of the spray current, and of the charge and size of the resulting droplets on the flow rate and liquid properties (electrical conductivity K, viscosity μ, liquid-gas surface tension γ, density ρ, and permittivity $\beta\epsilon_0$, ϵ_0 being the vacuum permittivity) is satisfactorily described in the case of liquids with sufficiently high values of the electrical conductivity and viscosity. The influence of the voltage and needle electrode geometry on the spray current for the case of less conducting and viscous liquids as well as the stability limits of the cone-jet mode are other problems that have not been sufficiently well understood.

Liquid motions inside Taylor cones which have been ignored in previous studies on electrosprays can be of some relevance for the understanding of the above-mentioned unsolved problems. These motions are driven by (1) the tangential electrical stress acting on the liquid-gas interface and (2) the flow rate injected through the electrified needle.

The tangential electrical stress $\tau_{r\theta}$ acting on the conical gas-liquid interface which in typical electrospray experiments is radial and pointing towards the origin is given by

$$\tau_{r\theta} = \epsilon_0 (E_\theta^o - \beta E_\theta^i) E_r , \tag{1}$$

where (r, θ, ϕ) are polar spherical coordinates, see Fig. 1, E_θ and E_r are the normal and tangential (in the r direction) components of the electric field, and superscripts o and i refer to the outer and inner (liquid) media, respectively. Except perhaps in the small transition region between the cone

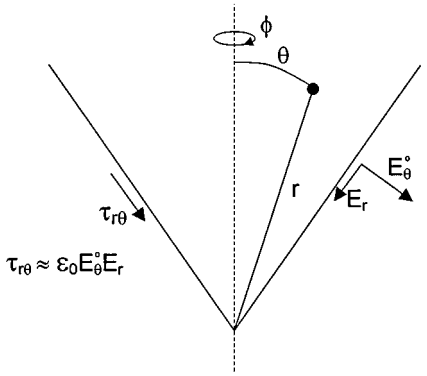

FIG. 1. Spherical coordinates and boundary conditions at the cone surface.

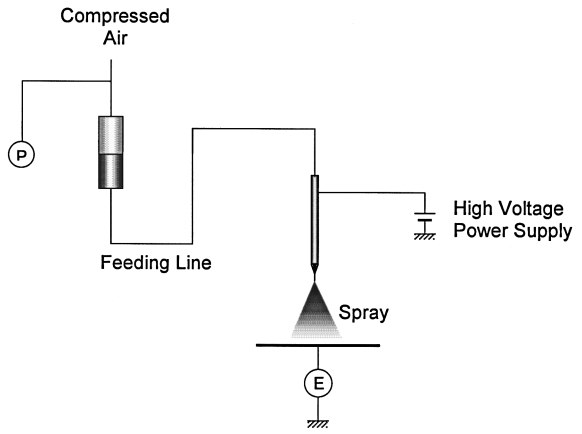

FIG. 2. Sketch of the experimental setup.

and jet, the electrical relaxation time is small compared to the hydrodynamic time of the liquid motion. Whether this condition is fulfilled in the transition region is still a matter of controversy. As a consequence, the liquid bulk is quasineutral in the upstream part of the meniscus, therefore charges are confined to a very thin layer adjacent to the liquid-gas interface. The thickness of the surface layer, of the order of Debye's length, is always small compared to any other characteristic length of the liquid motion. Moreover, the shielding effect of the charged layer at the surface leads to the well known condition $\beta E_\theta^i \ll E_\theta^o$, and, therefore, expression (1) becomes

$$\tau_{r\theta} = \epsilon_0 E_\theta^o E_r . \tag{2}$$

When highly conducting liquids are electrosprayed there is no noticeable motion different from the pure sink flow corresponding to the imposed value of the flow rate Q. In these cases, E_r is practically zero and therefore $\tau_{r\theta}$ is negligible. When the conductivity decreases, the tangential electrical stresses at the surface and consequently the liquid velocity there increase. A recirculating meridional motion, towards the apex along the generatrix and away from it along the axis, which was reported by Hayati, Bailey, and Tadros [20], appears if the characteristic velocity induced by the electrical stress is larger than that due to the flow rate. In addition to the meridional motion, an intense swirl is observed when liquids with very small values of both K and μ are electrosprayed [21–23].

II. EXPERIMENTAL OBSERVATIONS

The experimental setup is basically sketched in Fig. 2. Liquid contained in a small reservoir is forced by pressurized air through a narrow Teflon tube [inside diameter (i.d.)$\simeq$0.32 mm] whose length ranges from 20 to a few meters. Narrower silica tubes with diameters of 25, 50, and 100 μm are sometimes used to increase the pressure drop along the feeding line. The tube ends up at a charged capillary needle [inside diameter i.d.$\simeq$0.7 mm, outside diameter (o.d.)$\simeq$1 mm] connected to an electric potential of several kilovolts relative to a perpendicular flat ground electrode located to a distance of a few centimeters from the end of the needle.

Within the range of the experimental values, the flow rate Q varies linearly with the pressure difference across the feeding line ΔP, $Q = a\Delta P$. The dimensional constant a is found from calibration of Q and ΔP. ΔP is measured with a mercury manometer, and the flow rate is found by measuring the velocity of an air bubble introduced on purpose into the feeding line. Once constant a is known the measured value of ΔP directly yields the value of Q. The mass flow rate injected through the needle is approximately the same as that emitted from the cone vertex since the evaporated mass flow rate from the conical meniscus is much smaller than the injected flow rate Q. In all experiments the cone jet was operated at atmospheric pressure and room temperature. Then, ΔP ($\Delta P = P_0 - P_a$, P_0 being the stagnation pressure in the reservoir) and the needle voltage yielded by a BERTAN 250B-10R high voltage power supply are the control variables in the experiment. The current emitted from the cone is collected at the ground electrode and measured by a Keithley picoammeter. Surface tension has been measured by both the plate and ring methods with a tensiometer KRUSS. The electrical conductivity of the liquids has been measured by using a Microprocessor Conductivity Meter LF 3000 from WTW with an LR001/T cell also from WTW. Alternatively, we have measured the liquid conductivity following a method suggested in Ref. [12].

Polystyrene particles with diameter $d_p = 5$ μm and density $\rho_p = 1050$ kg/m^3 have been introduced into the liquid to observe the flow. In order to avoid an entanglement of pathlines which could blur the photographs, the concentration of polystyrene particles in the liquid must be small. On the other hand, flow visualization would not be possible if the particle concentration is too low. A Nikkon optical microscope up to 120$\times$ magnification factor has been used to obtain a detailed view of the flow pattern. Illumination of the meniscus is critical for a correct observation of the particle pathlines. In this respect, the unavoidable brightness due to the conical geometry of the meniscus must be minimized in order to improve the contrast of the image and to obtain a uniform illumination inside the meniscus. Best conditions have been achieved by using three different light sources. Two of them are symmetrically located with respect to the observation axis in such a way that this axis forms an angle of approximately 135° with the light rays impinging on the meniscus, see Fig. 3. Sometimes, an optical fiber whose end is located inside the needle is also used to illuminate the meniscus from inside.

The picture in Fig. 4 results from a superposition of several consecutive video frames showing the projections of the particle pathlines on the meridional plane of the Taylor cone orthogonal to the observation axis. In this first experiment, the liquid used is propylenglycol doped with a small amount of hydrochloric to enhance its conductivity ($K = 0.015$ S/m). For flow rates of the order of 10^{-12} m^3/s the resulting motion is purely meridional. Note that only fluid particles lying close to the surface are ejected through the jet while the rest recirculates towards the apex along the generatrix and away from it along the axis. Therefore the two flows are separated by the dividing stream surface passing through the stagnation point located at the axis at a certain distance from the tip. Our observations show that the flow pattern inside the meniscus remains essentially meridional when liquids with sufficiently high values of both viscosity

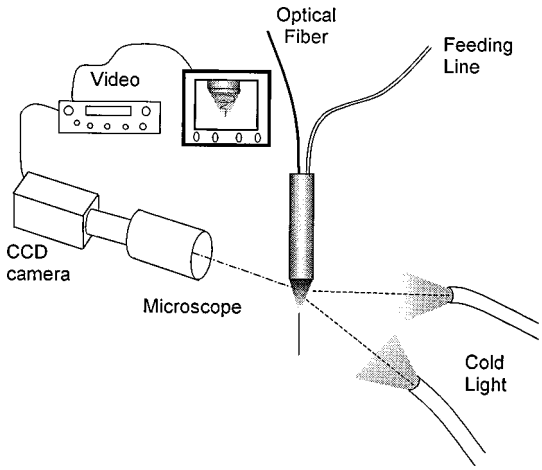

FIG. 3. Illumination setup for recording liquid motion in the Taylor cone.

and electrical conductivity are used.

In contrast, pictures in Figs. 5 and 6 show particle pathlines observed when liquids with lower values of both the electrical conductivity and viscosity (the case of liquid paraffins and some alcohols) are electrosprayed. Ethanol as purchased ($K=5\times10^{-5}$ S/m) was the liquid used in the experimental results shown in Figs. 5 and 6. The measured flow rate was $Q=6.3\times10^{-10}$ m^3/s. Trajectories of particles located near the axis are shown in Fig. 5 while Fig. 6 shows some other pathlines located closer to the cone surface. As it can be deduced from the helical trajectories in the picture, the resulting flow is a combination of a meridional motion,

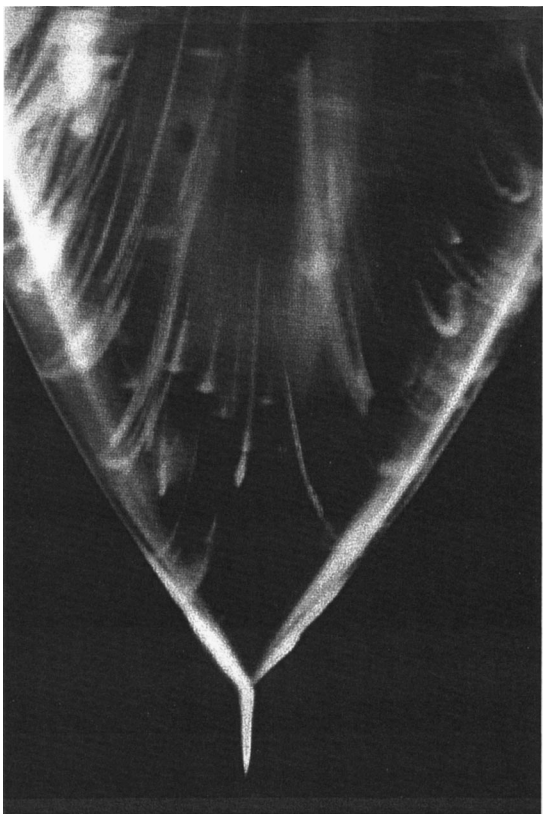

FIG. 4. Conical projections on a meridional plane of particle pathlines in an electrified meniscus of propylenglycol.

as in the previous case, and an intense azimuthal one (swirl).

Since the density of liquid and particles is different, one should wonder if the particle pathlines shown in Figs. 4–6 are actually fluid pathlines. The degree of coupling between the fluid and particle dynamics is measured by the Stokes number which is defined as the viscous to convective time ratio

$$S=\frac{t_v}{t_c}=(\rho_p-\rho)\,\frac{d_p v}{18\mu}, \tag{3}$$

where

$$t_v=(\rho_p-\rho)d_p^2/(18\mu), \quad \text{and} \quad t_c\sim d_d/v, \tag{4}$$

and v is here the liquid velocity relative to the particle. Clearly, the smaller the Stokes number the lesser is the difference between the fluid and particle motions. The maximum velocities observed in electrospray experiments are obtained when the less conducting and viscous liquids are electrosprayed. For heptane ($\rho=684$ kg/m^3 and $\mu=3.9\times10^{-4}$ kg m^{-1} s^{-1}), which is the less favorable case, we have measured velocities inside the cone of the order of 1 cm/s (see Sec. IV), so that, the Stokes number is as low as 10^{-4} and particles follow very accurately the fluid motion.

III. SPONTANEOUS SWIRL APPEARANCE IN LIQUID CONES

Pictures in Figs. 5 and 6 show unambiguously the existence of an intense swirl in Taylor cones. Independently of the surface finished at the needle's end and the injection conditions, this flow pattern appears whenever a liquid of very low viscosity and electrical conductivity is electrosprayed in the cone-jet mode. Since there is no apparent cause leading to swirl (the electrical tangential stress on the cone surface is radial) one must conclude that the swirling component of the velocity field appears spontaneously.

Spontaneous appearance of swirl in liquid motions with conical geometry driven by a tangential stress on the cone surface of the form

$$\tau_{r\theta}\sim r^{-2} \tag{5}$$

has been investigated in Refs. [22,23]. In these works, the viscous flow induced by a tangential stress of the form given in Eq. (5) is described in terms of the conical similarity class of exact solutions of the Navier-Stokes equations in such a way that the mathematical problem is reduced to the integration of a nonlinear system of three ordinary differential equations for the dimensionless stream function, azimuthal velocity, and pressure,

$$\psi(x)=\frac{\Psi(r,x)}{\nu r}, \quad \Gamma(x)=r v_\phi(r,x)\sin\,\theta/\nu, \tag{6}$$

$$\Pi(x)=\frac{r^2[p(r,x)-p_\infty]}{\rho\nu^2}, \quad x=\cos\,\theta, \quad 0\leqslant\theta\leqslant\alpha, \tag{7}$$

with appropriate boundary conditions, α being the cone semiangle. The results of this nonlinear problem show that if the Reynolds number of the flow based on the radial velocity

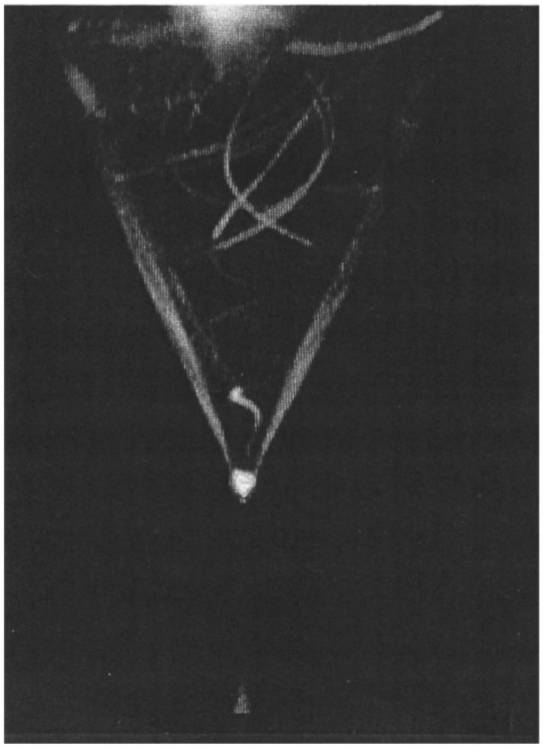

FIG. 5. Conical projections on a meridional plane of particle pathlines in an electrified meniscus of ethanol. Near-axis trajectories.

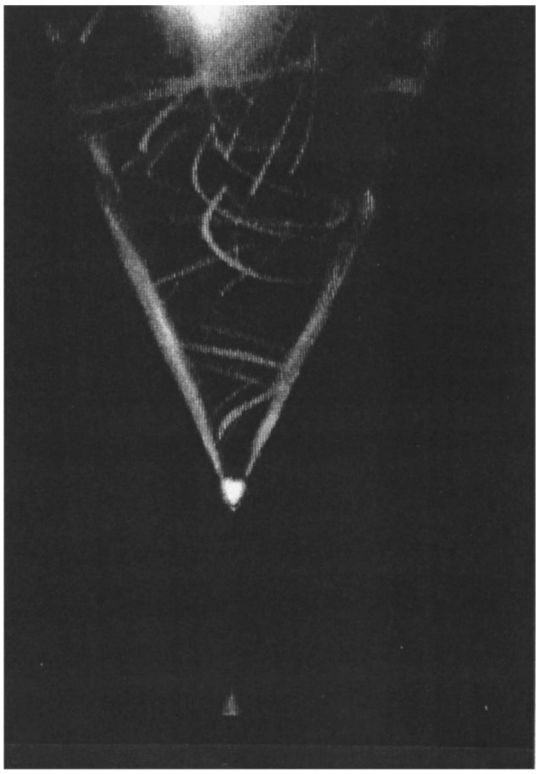

FIG. 6. Conical projections on a meridional plane of particle pathlines in an electrified meniscus of ethanol. Pathlines close to the liquid conical surface.

at the cone surface is less than a critical value Re=Re* (Re*=6.92 for $\alpha=45°$), $\Gamma(x)$ is identically zero everywhere and the motion is purely meridional while if the Reynolds number is larger than the critical one there are two mathematical solutions: one with $\Gamma=0$ everywhere, which is unstable, and the other with nonzero Γ which is found to be stable [23]. Spontaneous swirl is therefore due to bifurcation in the primarily pure meridional motion of a viscous liquid. The instability mechanism may be explained on the grounds that at sufficiently small Reynolds number any small upstream perturbation in the angular momentum is damped downstream by the action of viscosity. At higher Reynolds numbers any small perturbation of the angular momentum of the fluid is conserved along the converging flow (small damping rate) and consequently the angular momentum of the fluid increases as it approaches the axis [22,23]. It should be noted that the bifurcation occurs at a relatively low value of the Reynolds number.

Although in cone-jet electrospraying the tangential electrical stress is much more accurately described by a law of the form $\tau_{r\theta}\sim r^{-5/2}$ than that given by Eq. (3), see Ref. [15], it seems plausible to assume that the liquid motions inside Taylor cones will not deviate qualitatively much from the behavior previously described. Since the values of the electrical conductivity and viscosity of different liquids can differ in several orders of magnitude, the experimental conditions met in electrosprays range from very small values of the Reynolds number for which the creeping motion is purely meridional to moderately high values (in spite of the smallness of the electrified menisci, typically 1 mm), but larger than the critical value, for which the flow presents an azimuthal velocity component in addition to those of the meridional motion.

IV. ESTIMATES OF RELEVANT FLOW QUANTITIES

Electrical tangential stresses on the liquid surface give rise to a characteristic velocity U which can be larger or smaller than the order of magnitude of the sink velocity Q/L_c^2, L_c being the characteristic meniscus length (of the order of the needle diameter). The order of magnitude of the velocity U can be obtained from a balance of the viscous and electrical stresses at the gas-liquid interface

$$\tau_{r\theta}=\epsilon_0 E_\theta^o E_r\sim \mu U/L_c\,. \tag{8}$$

Clearly, meridional recirculating flow appears when $U \geqslant O(Q/L_c^2)$.

Following Ref. [15], we will assume that at the gas-liquid interface the normal component of the electrical field is of the order of the one given by Taylor [10],

$$E_\theta^o=\left(\frac{\gamma}{\epsilon_0 r\,\tan\,\alpha}\right)^{1/2}\sim\left(\frac{\gamma}{\epsilon_0 r}\right)^{1/2}. \tag{9}$$

Assuming also that the charge is transported by conduction inside the cone, we have

$$E_r=\frac{I}{2\pi(1-\cos\,\alpha)Kr^2}\sim\frac{I}{Kr^2}, \tag{10}$$

where I is the spray current. Introducing Eqs. (9) and (10) into Eq. (8) one easily arrives at

$$\tau_{r\theta}=-\left[\frac{\epsilon_0\gamma I^2}{2\pi^2(1-\cos\alpha)^2\tan\alpha K^2}\right]^{1/2}r^{-5/2}=-\Theta_{5/2}r^{-5/2}, \tag{11}$$

and

$$U\sim\left(\frac{\gamma\epsilon_0 I^2}{L_c^3K^2\mu^2}\right)^{1/2}, \tag{12}$$

which yields the order of magnitude of the velocities induced by the electrical stresses acting on the liquid surface as a function of the liquid properties, the needle diameter, and the current emitted by the spray. Therefore the typical value of the flow velocity can be known from a measurement of the current intensity emitted from the meniscus.

Clearly, the above result is valid as long as the Reynolds number defined as

$$\mathrm{Re}=\rho UL_c/\mu \tag{13}$$

is smaller than, or the order of, unity. If the Reynolds number of the flow is large, there is a viscous boundary layer of thickness $\Delta\sim L_c/Re^{1/2}\ll L_c$ adjacent to the liquid-gas interface. Outside this layer viscosity is negligible. Since the shear electrical stress is transmitted by viscosity, we have

$$\tau_{r\theta}\sim\mu\frac{U}{\Delta}\sim\mu\frac{U}{L_c}\mathrm{Re}^{1/2}\sim\left(\frac{\rho\mu U^3}{L_c}\right)^{1/2}, \tag{14}$$

and

$$U\sim\left(\frac{L_c\tau_{r\theta}^2}{\rho\mu}\right)^{1/3}\sim\left(\frac{\epsilon_0\gamma I^2}{\rho\mu K^2L_c^4}\right)^{1/3}. \tag{15}$$

The relative importance of the charge convection mechanism can now be estimated. The charge per unit time convected along the surface and the convected to total current ratio are given, respectively, by $\epsilon_0E_\theta^oUL_c$ and $\epsilon_0E_\theta UL_c/I$. Using Eqs. (9) and (12) the convected to total current ratio is given by $\gamma\epsilon/(K\mu L_c)$ which is a very small number for liquids with high viscosity and conductivity. On the other hand, using Eqs. (9) and (15), the convected to total charge ratio is given by $(\gamma\epsilon_0/L_c)^{5/6}(K^2\rho\mu I)^{-1/3}$. The maximum value of this ratio that we have found in electrospray experiments of liquids with low viscosity and low conductivity is of the order of 0.1; that is, charge conduction is the dominant transport mechanism in the cone since convection of charge represents at most 10% of the total current.

Let us now estimate the order of magnitude of the velocity flow in two typical electrospray experiments. In the first case, the liquid electrosprayed was octanol doped with a small amount of hydrochloric acid to enhance its electrical conductivity. Relevant properties of the liquid sample were $K=1.13\times10^{-2}$ S/m, $\rho=827$ kg/m, $\mu=7.2\times10^{-3}$ kg/(ms), and $\gamma=0.024$ N/m. A current of $I=1.39\times10^{-7}$ A was measured when a flow rate of $Q=1.27\times10^{-11}$ m^3/s was electrosprayed. Using the above data and taking $L_c=1$ mm like the diameter of the needle used, expressions (12) and (13) yield $U\sim0.24\times10^{-2}$ cm/s, $\mathrm{Re}\sim2.7\times10^{-3}$, and $Q/L_c^2\sim0.13\times10^{-2}$ cm/s. The flow pattern of this creeping flow ($\mathrm{Re}\ll1$) is entirely similar to the one shown in Fig. 4. It consists of a purely meridional flow where the liquid closer to the surface is ejected through the jet while the rest recirculates moving away the apex along the axis.

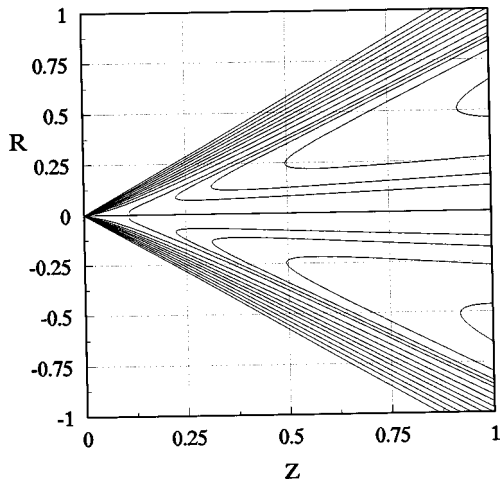

FIG. 7. Streamlines in the meridional plane corresponding to a conical creeping flow. The (R,Z) cylindrical coordinates are dimensionless and the origin has been taken at the cone vertex.

In the second experiment, we have electrosprayed heptane doped with a small amount of Stadis 450 [$K=3.16\times10^{-6}$ S/m, $\rho=684$ kg/m, $\mu=3.9\times10^{-4}$ kg/(ms), and $\gamma=0.021$ N/m]. Note that the values of the viscosity and conductivity are in this case much smaller than in the previous case. The measured current was $I=2\times10^{-8}$ A with a flow rate of $Q=3.86\times10^{-10}$ m^3/s. Using these data in expressions (15) and (13), we arrive at $U\sim3$ cm/s, $\mathrm{Re}\sim53$, and $Q/L_c^2\sim0.4$ mm/s. In this relatively high Reynolds number flow, viscous effects are restricted to a thin layer adjacent to the surface small compared to the dimensions of the meniscus ($\sim\frac{1}{7}$ mm) and the flow pattern of the motion is like those shown in Figs. 5 and 6: a vigorous swirl superimposed on the meridional motion.

V. MODELING OF FLOWS INSIDE TAYLOR CONES

Actual flows inside Taylor cones can be adequately described using self-similar conical solutions in two limit cases: high and small values of the Reynolds number. The simpler case corresponds to the limit $\mathrm{Re}\ll1$ for which the inertial term in the Navier-Stokes equations is negligible and the resulting equations are linear. Therefore the resulting flow can be obtained by superposition of a self-similar, zero flow rate, recirculating flow generated by an electrical stress at the surface with the form given in Eq. (11), and the flow due to a sink point located at the origin. Mathematically, such a flow which is self-similar has been reported in Ref. [24]. Figure 7 shows meridional streamlines in the [$R=(r/L_c)\cos\theta$, $Z=(r/L_c)\sin\theta$] cylindrical coordinates for a value of the dimensionless flow rate $Q\mu/(4\pi\Theta_{5/2}L_c^{1/2})=0.06$, and a cone semiangle $\alpha=49.3$, which corresponds to the angle given by Taylor [10]. Note the qualitative similarity between the particle pathlines in Fig. 4 and the streamlines in Fig. 7. As in Fig. 4, the dividing streamline separates the flow ejected through the jet from a recirculating flow.

In the limit Re$\gg$1, Fernández-Feria *et al.* [25] analyzed the conical flows generated by a tangential stress at the cone surface of the form

$$\tau_{r\theta} = -\Theta_n r^n, \tag{16}$$

where Eq. (11) is a particular case for $n=-\frac{5}{2}$. The structure of the flow, which is much more complex than in the case of low Reynolds numbers, consists of a viscous boundary layer at the cone surface which transmits the shear and sets the rest of the liquid cone in motion. Outside the surface boundary layer the motion is inviscid and can be represented mathematically by a meridional stream function and an azimuthal velocity of the form

$$\Psi(x,r) = r^m F(x), \quad 1 \leqslant \cos\theta \leqslant \cos\alpha, \tag{17}$$

$$v_\phi = r^{m-2}\Omega(x)/(1-x^2)^{1/2}. \tag{18}$$

For $n=-\frac{5}{2}$, it is found that $m=\frac{10}{13}$ and $\Omega(x)\neq 0$ at some point x of the flow field. Finally, the inviscid motion is singular at the axis and must be regularized through a near-axis swirling boundary layer [26].

The analysis yields the flow field as a function of the tangential stress and the liquid properties, in particular, the velocity of the liquid at the gas-liquid interface which can be tested in future experimental measurements. Also, as observed in electrospray experiments, Figs. 5 and 6, this analysis shows the existence of a swirl inescapably joined to the meridional flow. However, it should be mentioned that contrary to the case of small Reynolds number, the Re$\gg$1 problem is nonlinear and the superposition principle cannot be applied. Therefore the above zero flow rate conical solution becomes invalid in a region close to the cone apex where the sink flow velocities are comparable to or larger than the velocities induced by the electrical stress.

VI. CONCLUSIONS

It has been shown that flows at high and small Reynolds numbers occur in electrified liquid cones. The structure of the flow depends strongly on the conductivity and viscosity of the liquid. The tangential electrical stress acting at liquid-gas surface generates a recirculating meridional motion towards the vertex along the conical surface and away from it along the cone axis. For highly conducting and viscous liquids, the motion in the cone is essentially that corresponding to a sink flow while the strength of the recirculating motion increases when conductivity and viscosity decrease. For sufficiently low values of the conductivity and viscosity of the liquid the existence of an intense swirl (azimuthal motion) coupled to the meridional motion is always observed.

Estimates of the charge convection along the cone surface show that in the cone charge is mainly transported by conduction through the liquid bulk. Even in the case of the electrospraying of the less conducting liquids such as paraffins, the charge convection is only 10% of the total transport of charge.

Theoretical models of the flow using conical solutions have been developed in both regimes. The theoretical flow patterns agree well with those observed in the laboratory. In addition, some of the observed phenomena in the flow in an electrified conical meniscus such as meridional recirculating flow and the spontaneous appearance of swirl can be explained and predicted by the theoretical models.

ACKNOWLEDGMENTS

The authors thank M. A. Herrada for his valuable assistance with some numerical calculations. This work is supported by the Spanish Comisión Interministerial de Ciencia y Tecnología under Project No. PB96-0679-C02-02.

[1] M. Cloupeau and B. Prunet-Foch, J. Electrost. **22**, 135 (1989).
[2] A. M. Gañán-Calvo, Phys. Rev. Lett. **80**, 285 (1998).
[3] A. M. Gañán-Calvo and A. Barrero, J. Aerosol Sci. (to be published).
[4] A. J. Rulison and R. C. Flagan, J. Am. Ceram. Soc. **77**, 3244 (1994).
[5] E. B. Slamovich and F. F. Lange, in *Better Ceramics through Chemistry III Symposium*, edited by C. J. Brinker, D. E. Clark, and D. R. Ulrich (Materials Research Society, Pittsburgh, 1988), pp. 257–262.
[6] G. M. H. Meesters, P. H. W. Vercoulen, J. C. M. Marijnissen, and B. Scarlett, J. Aerosol Sci. **23**, 37 (1992).
[7] J. B. Feen, M. Mann, C. K. Meng, and S. F. Wong, Science **246**, 64 (1989).
[8] J. Zeleny, Phys. Rev. **3**, 69 (1914).
[9] J. Zeleny, Phys. Rev. **10**, 1 (1917).
[10] G. I. Taylor, Proc. R. Soc. London, Ser. A **280**, 383 (1964).
[11] J. Fernández de la Mora, J. Fluid Mech. **243**, 561 (1992).
[12] J. Fernández de la Mora and I. G. Loscertales, J. Fluid Mech. **260**, 155 (1994).
[13] A. M. Gañán-Calvo, J. C. Lasheras, J. Dávila, and A. Barrero, J. Aerosol Sci. **25**, 1121 (1994).
[14] J. M. Grace and J. C. M. Marijnissen, J. Aerosol Sci. **25**, 1005 (1994).
[15] A. M. Gañán-Calvo, J. Dávila, and A. Barrero, J. Aerosol Sci. **28**, 249 (1997).
[16] A. Gomez and K. Tang, Phys. Fluids **6**, 404 (1994).
[17] D. R. Chen, D. Y. H. Pui, and S. L. Kaufman, J. Aerosol Sci. **26**, 963 (1995).
[18] A. M. Gañán-Calvo, Phys. Rev. Lett. **79**, 217 (1997).
[19] A. M. Gañán-Calvo, J. Fluid Mech. **335**, 165 (1997).
[20] I. Hayati, A. Bailey, and Th. F. Tadros, Nature (London) **319**, 41 (1986).
[21] V. Shtern and A. Barrero, J. Aerosol Sci. **25**, 1049 (1994).
[22] V. Shtern and A. Barrero, Phys. Rev. E **52**, 627 (1995).
[23] V. Shtern and A. Barrero, J. Fluid Mech. **300**, 169 (1995).
[24] A. Barrero, A. M. Gañán-Calvo, and R. Fernndez-Feria, J. Aerosol Sci. **1**, 175 (1996).
[25] R. Fernández-Feria, J. Fernández de la Mora, M. Pérez-Saborid, and A. Barrero, J. Mech. Appl. Math. (to be published).
[26] R. Fernández-Feria, J. Fernández de la Mora, and A. Barrero, J. Fluid Mech. **305**, 77 (1995).